

Extraction of Mosaic Regions through Projection and Filtering of Features from Image Big Data

Seok-Woo Jang¹

¹ Department of Software, Anyang University
22, 37-Beongil, Samdeok-Ro, Manan-Gu, Anyang 14028, Korea,
swjang7285@gmail.com

Abstract. When uploading multimedia data such as photos or videos on social network services, websites, and so on, certain parts of the human body or personal information are often exposed. Therefore, it is frequent that the face of a person is blurred out to protect the portrait right of a particular person, and that repulsive objects are covered with mosaic blocks to prevent others from feeling disgusted. In this paper, an algorithm that detects mosaic regions blurring out certain blocks based on the edge projection is proposed. The proposed algorithm initially detects the edge and uses the horizontal and vertical line edge projections to detect the mosaic candidate blocks. Subsequently, geometrical features such as size, aspect ratio and compactness are used to filter the candidate mosaic blocks, and the actual mosaic blocks are finally detected. The experiment results showed that the proposed algorithm detected mosaic blocks more accurately than other methods.

Keywords: Video Analysis, Edge Extraction, Geometrical Feature, Filtering, Candidate Verification

1. Introduction

Recently, with the rapid development of mobile sensing, computer networks, high-definition cameras and artificial intelligence technologies, the amount of social multimedia data available is increasing explosively [1-5]. In particular, as smart mobile devices and location-based services are expanded, real-time location-based video data are actively used, and such digital image data are creating large-scale big data [6-10]. Additionally, related real application programs that can be used to effectively search and process such social multimedia data are diversely developed and utilized in various social computing fields [11-15].

In general, a color image includes valuable information but also includes information not preferred being exposed to other people. For example, Google Street View [16, 17] that can be used by ordinary people to freely search and confirm a map through an Internet browser sometimes exposes the face of a person or the license plate of a car, which is considered the personal information of a particular person. The service uses 11 lenses of 100 million pixels, which are captured in high quality to provide relatively detailed scenes such as bus routes, street structure and people.

However, in some cases, the street view service is too private, leading to a backlash and criticism of invading privacy. In fact, when she entered the address of a woman in

California into a street view search window, she saw a cat being raised through her living room window. Besides, the view of women who are on the street or sunbathing in bikinis has been shown in the street view, which has increased the controversy over whether or not human rights violations are excessive among Internet users. As such, as social video services that can be usefully utilized in real life are developed, it is expected that image big data exposed to personal information will also increase exponentially.

In addition, in the process of searching blogs on the Internet, uploaded pictures or video clips sometimes include the face or some body part of a person who does not wish to be exposed. In other words, the Internet is also causing dysfunction by providing users with indiscriminately exposed video contents that require social control. Video contents that contain personal information and exposed human body parts or harmful contents are easily exposed and distributed to children and adolescents who lack judgment and restraint without any sanctions. It is a big problem. Furthermore, if various video contents, including exposed human body parts, are made available to the public, the mental damage and side effects to the parties concerned are expected to be beyond imagination.

Nowadays, some websites or mass media have access to articles on the damage of video content that exposes personal information, so the side effects of this do not seem to be apparent. However, not long after, the existing mega-class Internet will bring a quantum jump to speed and it will be replaced by a Giga-class Internet with a different communication life. Video content will also explode. Therefore, it is clearly expected that this kind of various harmful video contents will overflow in the near future because video data can be viewed in a much more natural and faster environment than now.

Accordingly, mosaic blocks are frequently used nowadays to blur out such areas [18]. In particular, particular attention is paid to induce the generated mosaic blocks to be harmonized with the surrounding blocks. In addition, in the image processing fields related to detection of harmful and adult images [19, 20] and in the real application fields related to computer vision and pattern recognition, to effectively determine whether or not the given input image includes exposed body parts not preferred by users, an attempt is being made to detect the image parts processed with grid-type mosaic blocks [21].

The existing studies associated with the field where mosaic-processed blocks are automatically detected from such digital image data can be found in the related references. In [22], the edge was detected from the input image, and the candidate mosaic blocks were generated based on the detected edge. Then, the actual mosaic blocks were finally selected through the filtering process that uses geometrical features. In [23], to accurately detect mosaic blocks, the fuzzy c-means clustering algorithm was used. As far as this method is concerned, the Sobel edge was detected from the input image, the clustering features were extracted, and the fuzzy c-means clustering was applied to distinguish between general image blocks and grid-type mosaic blocks. In [24], the edge was detected from the image, and the template matching was used to detect the candidate mosaic domains. Finally, a support vector machine (SVM) was used to select the final actual mosaic blocks. In [25], a method is proposed that analyzes mosaic features in detail using a template matching-based method and then detects mosaics in the spatial domain. This method employs two strategies to speed up the detection of mosaics: a new template matching strategy and preprocessing of edge

images. In addition to such methods, many methods are used to effectively detect mosaic blocks [26].

Although the existing approaches described above are capable of extracting mosaic-processed blocks to a certain extent, they are not sufficient in terms of accuracy. To this day, studies related to algorithms generating and detecting mosaic blocks are relatively not actively conducted. Accordingly, in this paper, a new algorithm that can be used to effectively detect grid-type mosaic blocks based on the Canny edge projection was proposed. In this paper, the mosaic blocks used to blur out particular human body parts in harmful or adult images were selected as the main detection targets. In general, although the mosaic blocks used in harmful images may vary in size depending on the block to be blurred out, such mosaic blocks tend to be based on a simple format rather than a complicated format. Although there are harmful images that include blurring or virtual object insertion instead of grid-type mosaic blocks, most harmful images tend to use mosaic blocks to this day.

The methods introduced in this study have the following main contributions compared to other existing methods: First, the proposed method detected edges from color images being entered and then newly defined an edge that is connected continuously for more than a certain length in horizontal and vertical directions as a line edge. The line edge introduced in this paper can be usefully used as a new feature in object detection and image segmentation. Second, the proposed method was to project a line edge and then compare the frequency of the projected edges to effectively detect the boundaries of the blocks forming the mosaic. Third, the proposed algorithm improves the accuracy of final mosaic area detection by extracting geometric features such as size, aspect ratio, and density and robustly filtering candidate areas of mosaic detected in the previous phase.

Figure 1 shows the overall flow chart of the mosaic detection algorithm proposed in this paper. As shown in Figure 1, the proposed algorithm initially detects the Canny edge features from the input color image, then extracts the line edge over a certain length. Candidate regions of the mosaic are then detected based on horizontal and vertical line edge projection. Subsequently, the final actual grid-type mosaic regions are detected by removing the non-mosaic region through robust filtering of candidate mosaic regions using geometrical features such as size, aspect ratio, and compactness.

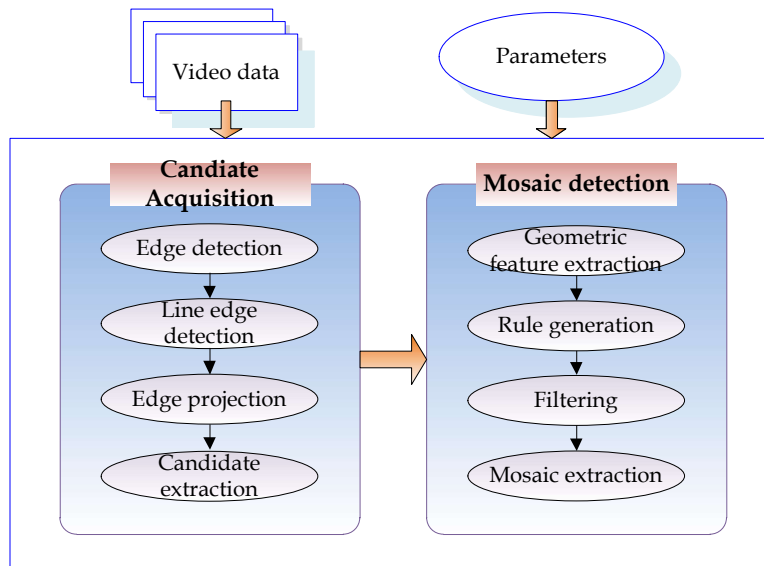


Fig. 1. Overall flowchart of the proposed method.

In this paper, we robustly detect the mosaic area in blocks to effectively protect specific parts of the human body exposed from the input images. This is to accurately detect images harmful to adolescents or children by detecting grid-type mosaic areas. Therefore, the proposed system does not recognize the detected mosaic region, nor does it remove the detected mosaic or generate a new mosaic. In other words, the suggested algorithm extracts a grid-type mosaic feature that can be used to detect harmful images along with color, edge, skin region, texture, contour, and shape features.

The remaining chapters of this paper are constructed as follows. In Chapter 2, diverse existing studies conducted in related to the mosaic detection methods used in the image processing and video analysis fields are described. In Chapter 3, the method for extracting the candidate mosaic blocks through extracting the edge and using the horizontal and vertical projections of the extracted edge is described. In Chapter 4, the method that uses geometrical features to remove the non-mosaic blocks from the candidate mosaic blocks and filtering the actual mosaic blocks is described. In Chapter 5, the results of an experiment conducted to compare and evaluate the performance of the proposed mosaic detection method are described. In Chapter 6, the conclusion of this paper is described and the future research direction is described as well.

2. Related Work

As information communication technologies, miniaturized displays, and inexpensive storage devices make progress, the volume of available social multimedia data is increasing exponentially [27-33]. However, such video data usually include valuable

information, but also include information not preferred being exposed to other people such as the face or human body part of other people. Accordingly, to determine whether or not given video data include information not preferred by users, an attempt is being made to detect the image parts processed with grid-type mosaic blocks. Therefore, in recent years, the need for a technique for robustly detecting such mosaic regions and effectively filtering out the detected mosaic areas has been raised. Various existing methods related to the detection of grid-type mosaics, which are introduced in related documents, are as follows.

As far as the method using the edge [22] is concerned, to accurately identify the harmfulness of the input color image, a technique detecting the grid-type mosaic blocks in an adult image was proposed. In this method, to detect the grid-type mosaic blocks mainly used in adult video content, an algorithm was conducted in two major phases: a phase where the candidate mosaic blocks were detected and a phase where the candidate mosaic blocks were verified. Initially, in the phase where the candidate mosaic blocks were detected, the edge was detected from the input color image, a mosaic map was generated and binarized based on the detected edge image, and the final candidate mosaic blocks were detected. In the phase where the candidate mosaic blocks were verified, the mosaic map value of the candidate mosaic blocks and the geometrical features of the candidate mosaic blocks were used to detect the final mosaic blocks. The experimental results of this method showed that the proposed method is generally superior to the adult image, but shows slightly higher false detection on non-mosaic images. Most of the candidate regions using mosaic maps included mosaics, but false or non-detection occurred somewhat because a verification method using a simple threshold was used. Further research is needed on the part of the verification of candidate areas. The overall performance of the suggested edge-based mosaic detection algorithm was not bad. Figure 2 shows the overall flow diagram of the edge map-based mosaic detection approach.

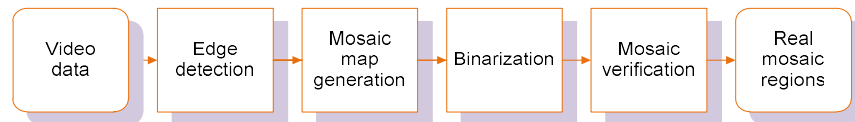


Fig. 2. Overall flowchart of the edge-based method.

As far as the method using the clustering [23] is concerned, a new mosaic block detection method that detects mosaic blocks based on the fuzzy c-means clustering was proposed. Image recognition techniques are commonly applied to detect degraded video in television viewing systems. Mosaic signals, which degrade the quality of the video, occur easily in TV signals. This approach consisted of three major phases. In the first phase, the input video is captured by the digital TV receiver and decoded into video frames. The input image is then converted into the gray-scale image and the Sobel edge detection algorithm was applied to the input color image to acquire the edge image. In the second phase, by using the extracted edge as the target, the clustering features of the fuzzy c-means clustering algorithm were extracted. In the Sobel edge detection algorithm, an adaptive thresholding is used to convert gray-scale images to binary images. Subsequently, features for the clustering algorithm are extracted by the direct

selection method. In the third phase, the fuzzy c-means clustering was applied, and the mosaic blocks were distinguished from all general image blocks. In other words, according to the classification result, mosaic blocks of the image are detected. If the number of mosaic blocks is higher than the predefined threshold, the image is considered a frame with mosaic blocks. Based on the experimental results of this method, it was specified that the algorithm used in this method was able to distinguish the actual mosaic blocks relatively well and that the incorrect detection rate was comparatively low. In particular, the existing mosaic detection method has a disadvantage that it is not possible to distinguish between Chinese characters and actual mosaic, but the proposed method detects the actual mosaic area more robustly. Figure 3 shows the overall flowchart of the fuzzy c-means clustering-based mosaic block detection method.

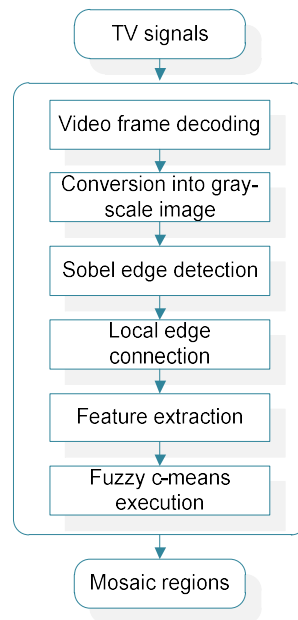


Fig. 3. Overall flowchart of the clustering-based method.

As far as the method using the macroblock [24] is concerned, a macroblock format was utilized to detect mosaic blocks. In general, as far as a digital video is concerned, mosaic blocks are expressed as one of the general phenomena resulting from video defects and are what lowers the quality of a video. Accordingly, restoring a video by detecting mosaic blocks is gradually becoming more important. In general, since a macroblock is the smallest synchronization unit used in video images, mosaic regions occur in the unit of macroblock. In this paper, a mosaic block detection method based on the macroblock's solid edge detection was proposed. The edge of an image is a collection of image pixels. The gray-scale of a pixel often varies greatly, and such collections of pixels are often closed curves. The curve concentrates most of the

information of the image. Therefore, extracting image edges is very important for recognizing and understanding the whole image. For this purpose, initially, the input color image was processed based on the Canny edge detection algorithm, and the edge image was acquired. Secondly, the binarized edge image was traversed based on the macroblock, and the solid edge of the macroblock was determined. In this study, solid edges are defined as clear edges in macroblocks and can be acted as the determination of mosaic blocks. In this method, depending on the edge detection result, the edge type of the macro block can be divided into five types. Finally, the mosaic block was determined based on the number of all the macroblocks' solid edges. In other words, if the number of mosaic macro blocks of a video frame is greater than the number threshold of macro blocks, this frame is indicated as a mosaic frame. The experimental results of this method showed the good performance of the proposed algorithm. Compared to the video mosaic detection method based on support vector machine [34, 35] and template matching [36, 37], the complexity is low, thus it is faster and does not require data training. Besides, the method is simple and efficient.

The quality of a video may be lowered by physical issues such as repeated projection, low-quality compression, decompression and defective chemical degradation of original recording data. It is gradually becoming more important to use broad-based digital media application programs to find a quality-degraded video. One general video defect is mosaic blocks where an original image information loss occurs due to a few squares combined together. As far as the template matching-based method [25] is concerned, a method for detecting mosaic defects in spatial and edge domains was proposed after specifically analyzing the characteristics of a mosaic defect. In this method, four even squares were initially detected, and the intersection points of the squares were selected as the mosaic macroblock (MMB)'s features. The mosaic consisted of various MMBs. Meanwhile, an automatic detection algorithm prompt and effective in an edge domain was proposed by analyzing the existing approach method. In this method, to increase the mosaic detection speed, two new tricks were selected: a new template matching strategy and the edge image pre-processing. The experimental results of this method showed the outstanding performance of the proposed algorithm. In the future, the idea of the proposed mosaic detection approach can be applied broadly to solve other problems for degraded video defect detection, such as digital dropout, betacam dropout, and so on.

In addition to the various methods described above, new methods related to mosaic detection are being continuously introduced [26]. Although the existing algorithms described above are capable of accurately detecting mosaic-processed blocks to a certain extent, they are relatively not sufficient in terms of accuracy. Also, existing methods have various constraints on the photographing environment or condition of the color image and the grid mosaic area. To this day, new studies related to image processing and pattern recognition algorithms that generate and detect grid-type mosaics to blur out target objects exposing personal information are not as actively conducted as other studies.

3. Extraction of Candidate Mosaic Blocks

The grid-type mosaic areas included in the input color image consist of mosaic blocks (MB). In general, such mosaic blocks demonstrate the following four characteristics. Initially, the pixels located within a mosaic block share the same color. Accordingly, no edge exists within a mosaic block. Secondly, mosaic blocks share the same size. In other words, both the horizontal length and the vertical length of the mosaic block are the same. Thirdly, mosaic blocks are adjacent to one another and form a cluster. Fourthly, no edge exists among adjacent mosaic blocks sharing the same gray value.

In this paper, initially, the Canny edge $CE(x, y)$ was extracted from the input image [38-42]. As far as a color image is concerned, since an edge is one of the important features for detecting mosaics, as the initial phase, to accurately extract an edge image is very important. In general, since the Canny edge demonstrates comparatively high accuracy in terms of finding the contour line, it is one of the most used edge detectors in the image processing and computer vision fields.

Canny edge extraction consists of four major steps. First, a Gaussian smoothing is applied to the input color image. Second, the Sobel operator is applied to the smoothed result image to obtain the edge strength map and the edge direction map. Third, non-maximum suppression is applied to create a thin-thickness edge map. Fourth, hysteresis thresholding is applied to remove false positives. In general, Canny edge extraction has the advantage of accurately detecting edges, while the algorithm is complicated and takes some time to execute. The horizontal and vertical masks used for Canny edge extraction in this paper are shown in Figure 4.

- 1	0	1	1	2	1
- 2	0	2	0	0	0
- 1	0	1	- 1	- 2	1

(a) Horizontal mask (b) Vertical mask

Fig. 4. Horizontal and vertical mask.

The proposed system detects edges connected continuously over TH_{line} pixels in the horizontal direction (0° or 180°) from the extracted canny edge, which are called horizontal line edge $LE_h(x, y)$ in this paper. Besides, edges continuously connected over TH_{line} pixels in the vertical direction (90° or 270°) are detected and named as vertical line edge $LE_v(x, y)$.

Then, as shown in (1), the vertical line edge $LE_v(x, y)$ is projected in the direction of the x axis. A set of x coordinates in which $Proj(x)$, which is the number of pixels accumulated through projection, is equal to or greater than TH_{accum} is obtained as shown in (3).

$$Proj(x) = \sum_{x=0}^W LE_v(x, y) \quad (1)$$

$$Proj(y) = \sum_{y=0}^H LE_h(x, y) \quad (2)$$

Similarly, as shown in (2), the horizontal line edge $LE_h(x, y)$ is projected in the y-axis direction. Then, a set of y coordinates in which $Proj(y)$, which is the number of pixels accumulated through the projection, is equal to or greater than TH_{accum} is acquired as shown in (4). In (1) and (2), W and H represent the width and height of the input image.

$$X_{accum} = \{x_1, x_2, \dots, x_m\} \quad (3)$$

$$Y_{accum} = \{y_1, y_2, \dots, y_n\} \quad (4)$$

X_{diff} , the difference among the adjacent x coordinates in group X_{accum} , and Y_{diff} , the difference among the adjacent y coordinates in group Y_{accum} are calculated as shown in (5) and (6), respectively. Then, of X_{diff} and Y_{diff} , the values having the highest frequency and the value having the lowest frequency are selected and determined as N and M of the mosaic blocks having a size equivalent to the $N \times M$ pixel size.

$$X_{diff} = \{x_k - x_{k-1} \mid x_k \in X_{accum}, k = 2, 3, 4, \dots, m\} \quad (5)$$

$$Y_{diff} = \{y_k - y_{k-1} \mid y_k \in Y_{accum}, k = 2, 3, 4, \dots, n\} \quad (6)$$

We select x coordinates where the difference between adjacent x coordinates in the set X_{accum} is N , and y coordinates where the difference between adjacent y coordinates in Y_{accum} is M , as shown in (7) and (8).

$$X_{mosaic} = \{x_k \mid x_k \in X_{accum}, (x_k - x_{k-1}) == N\} \quad (7)$$

$$Y_{mosaic} = \{y_k \mid y_k \in Y_{accum}, (y_k - y_{k-1}) == M\} \quad (8)$$

The minimum enclosing rectangle (MER) [43, 44] regarding the domain including all the locations (x, y) having a value included in X_{mosaic} as the input image's x coordinate and a value included in Y_{mosaic} as the input image's y coordinate are selected as shown in (9), and the defined MER is selected as the candidate mosaic block to be detected in this paper. In (9), (x_p, y_p) and (x_q, y_q) refer to the initial and final coordinates of the MER, respectively. The candidate regions of the grid-type mosaic defined as in (9) are used as the input data of the actual mosaic detection step, which is the next step.

$$MER_{mosaic} = \{x_p, y_p, x_q, y_q\} \quad (9)$$

Figure 5 shows the main process flow diagram for extracting the candidate mosaic blocks mentioned above.

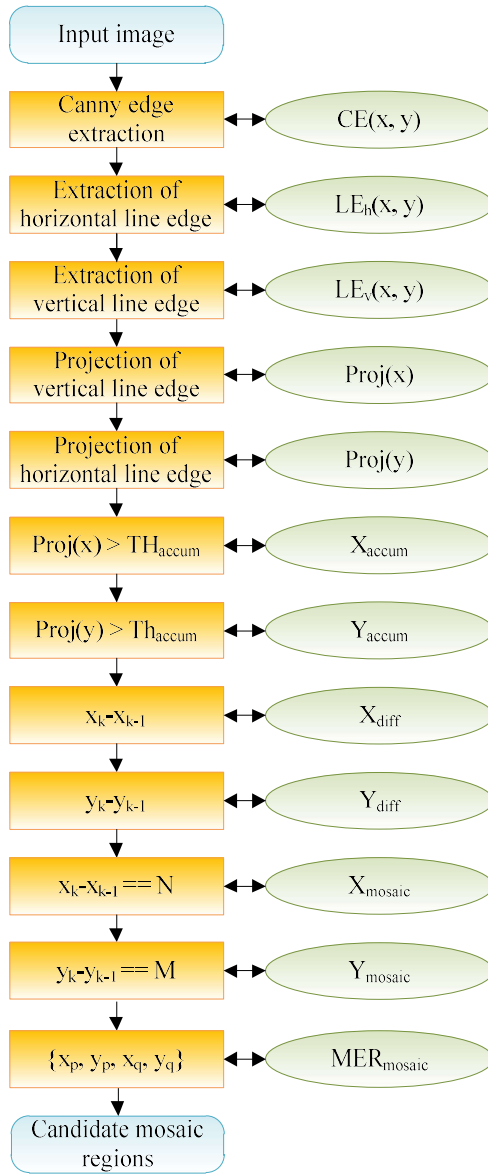


Fig. 5. Process flow diagram of detecting candidate mosaic areas.

4. Mosaic Detection through Filtering

In this paper, the geometrical features [45-50] are used to remove the candidate blocks determined to be non-mosaic blocks among the detected candidate mosaic blocks, and only actual mosaic regions are selected. The geometrical features F_{model} used for removing the candidate mosaic blocks are the size feature $size(R_i)$, the aspect ratio feature $aspect(R_i)$ and the compactness feature $compact(R_i)$ of the candidate mosaic blocks, and such features are defined and utilized as shown in equations (10) to (13).

$$F_{model} = \{size(R_i), aspect(R_i), compact(R_i)\} \quad (10)$$

$$size(R_i) = \frac{Num(R_i)}{W \times H} \quad (11)$$

$$aspect(R_i) = \frac{MER_h(R_i)}{MER_w(R_i)} \quad (12)$$

$$compact(R_i) = \frac{Num(R_i)}{MER_w(R_i) \times MER_h(R_i)} \quad (13)$$

In equations (10) to (13), F_{model} represents a feature model for the mosaic region that contains three geometrical features. R_i refers to the i -th region among the candidate mosaic regions extracted in the previous phase. W and H represent the horizontal length and the vertical length of the input color image, respectively. $Num(R_i)$ refers to the total number of pixels included within the candidate mosaic block R_i . Besides, $MER_w(R_i)$ and $MER_h(R_i)$ refer to the horizontal length and the vertical length, respectively, of the minimum enclosing rectangle included for candidate mosaic block R_i .

Initially, the candidate block's size feature $size(R_i)$ is used to effectively remove the too small candidate mosaic blocks. Usually, a candidate mosaic region having a small size is extracted when an unexpected noise is inserted in an input color image or when a small-sized object having line edges exists in the color image [51-54]. In other words, an area that is too small is not considered a grid-type mosaic. Mosaic blocks are usually used to mask areas of the exposed body in harmful images. In particular, it produces mosaic blocks of larger size rather than precisely fitting to the exposed body region. Therefore, candidate regions of relatively small size are removed from the candidate group of mosaics.

The aspect ratio feature $aspect(R_i)$ is used to effectively remove the non-mosaic blocks that too excessively lean toward one direction. Although grid-type mosaic blocks too excessively extended towards a particular direction may exist, such blocks are not frequently found in actual harmful or adult images. In other words, most of the exposed areas of the human body parts in the harmful image are located in the center of the input color image, and the shape of the corresponding area exists in a constant ratio in the horizontal direction and the vertical direction rather than in one direction.

The $compact(R_i)$ is used to remove the non-mosaic blocks having low compactness within the block. Usually, since there is no hole inside the grid-type mosaic area, the density of the region is high. Therefore, in the proposed method, when the density feature of the candidate mosaic region is relatively low, the candidate region is considered as the non-mosaic region and removed from the candidate mosaic group.

In this paper, as shown in (14), (15) and (16), the geometrical features defined above are applied to the candidate mosaic blocks, and the blocks having a threshold lower than the predefined threshold [55-58] are determined to be non-mosaic blocks and are removed from the candidate blocks. In (14), (15) and (16), TH_{size} , TH_{aspect} , and $TH_{compact}$ refer to the predefined threshold size, threshold aspect ratio and threshold compactness of the candidate mosaic block, respectively. In this paper, such threshold values are artificially defined in advance through the repeated experiments.

$$\begin{aligned}
 & \text{IF } (size(R_i) < TH_{size}) \text{ THEN} \\
 & \quad \text{eliminate } R_i \\
 & \text{ELSE} \\
 & \quad \text{select } R_i \text{ as a mosaic region}
 \end{aligned} \tag{14}$$

$$\begin{aligned}
 & \text{IF } (aspect(R_i) < TH_{aspect}) \text{ THEN} \\
 & \quad \text{eliminate } R_i \\
 & \text{ELSE} \\
 & \quad \text{select } R_i \text{ as a mosaic region}
 \end{aligned} \tag{15}$$

$$\begin{aligned}
 & \text{IF } (compact(R_i) < TH_{compact}) \text{ THEN} \\
 & \quad \text{eliminate } R_i \\
 & \text{ELSE} \\
 & \quad \text{select } R_i \text{ as a mosaic region}
 \end{aligned} \tag{16}$$

In this paper, the three features defined above are applied to the candidate mosaic blocks to remove all the blocks determined to be non-mosaic blocks, and the remaining blocks are finally determined to be the actual mosaic blocks.

Although it is possible that general mosaic blocks, for example, mosaic blocks used to blur out particular buildings or signs, can be removed due to geometrical features such as aspect ratio and size, since mosaic blocks that blur out body parts are set as the main detection targets in this paper, the geometrical features used in this paper are effectively operated. Figure 6 shows the overall flow of the approach for filtering candidate mosaic areas.

In the future, to further improve the performance of the proposed system, in addition to the features used in this paper, it is necessary to additionally define new features that can represent grid-type mosaics such as texture and smoothness features. There is also a need for an algorithm that accurately and quickly extracts the newly defined features from the input image. In particular, the proposed system should define the weights that indicate the importance of each feature, and it is also necessary to improve the performance of the proposed mosaic detection system by adaptively and automatically adjusting the weights according to the environment in which the image is taken.

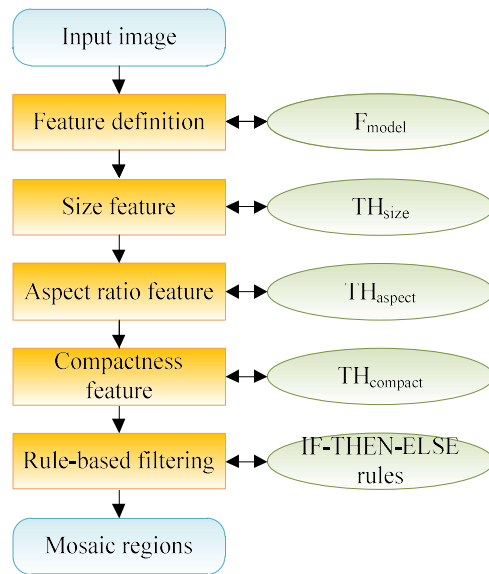


Fig. 6. Overall flow of the candidate filtering process.

5. Experimental Results

In this paper, the personal computer used for experiments consisted of Intel Core(TM) i7 2.83 GHz CPU and 8GB main memory, and is equipped with Windows 7 operating system. Microsoft's Visual Studio and OpenCV open-source computer vision library are used to implement the proposed algorithm. To comparatively evaluate the performance of the algorithm proposed in this paper, various types of indoor and outdoor input color images including grid-type mosaic blocks are collected and utilized. Such images are captured in diverse natural indoor and outdoor environments where no particular restrictions are set. Figure 7 shows an example of the input color images with grid-type mosaic regions.

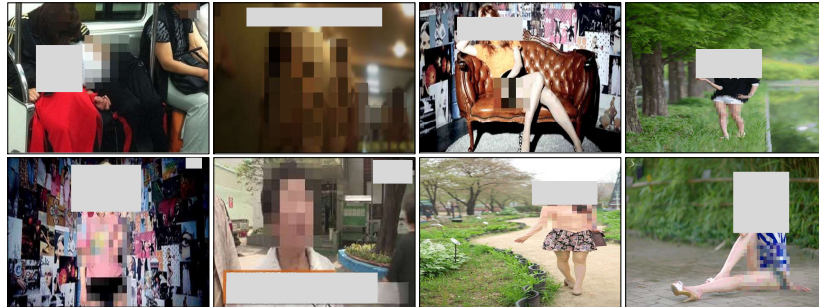


Fig. 7. Example of input images with mosaic.

Figure 8 (a) shows an input color image in which mosaic blocks exist, and Figure 8 (b) shows the result of the Canny edge features extracted from an input image. As shown in Figure 8 (a), there is a grid-type mosaic area near the center of the input image. In Figure 8 (b), it can be seen that the line-shaped edges are concentrated in the center of the image. As expected, Figure 8 shows that the Canny edge represents the object's appearance information relatively accurately.

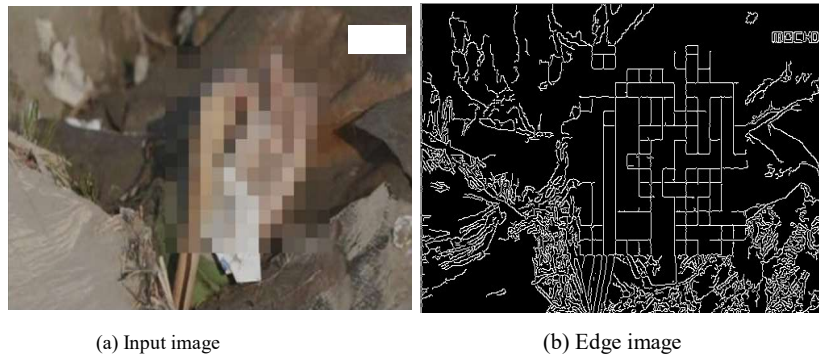
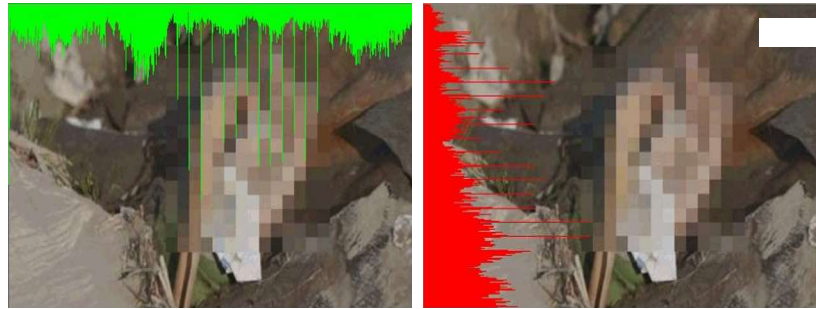


Fig. 8. Input image and edges.

Figure 9 (a) shows the histogram of horizontally projected line edges, and Figure 9 (b) shows the histogram of vertically projected line edges. As shown in Figure 9, it can be seen that the frequency of the histogram of the line edges is relatively high in the region where the grid-type mosaic blocks exist.



(a) Histogram of horizontally projected edges (b) Histogram of vertically projected edges

Fig. 9. Histogram of projected line edges.

Figure 10 shows the result of the actual mosaic blocks remaining after removing non-mosaic blocks from the candidate mosaic blocks through the application of geometrical features.

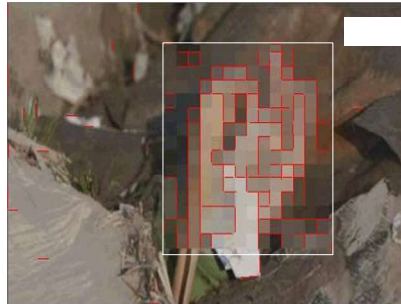


Fig. 10. Detected mosaic region.

In this paper, we used an accuracy measure defined as (17) and (18) to quantitatively evaluate the performance of the proposed mosaic detection algorithm [59-63]. In (17) and (18), N_{TP} indicates the number of mosaic regions accurately detected, N_{FP} represents the number of regions that are incorrectly detected as mosaic regions but not mosaic regions, and N_{FN} denotes the number of mosaic regions that are not detected. In (17) and (18), $R_{precision}$ represents a relative ratio of mosaic regions accurately detected among the entire mosaic regions detected from the input color image, and R_{recall} is a relative ratio of mosaic regions accurately detected among all mosaic regions present in the input image.

$$R_{precision} = \frac{N_{TP}}{N_{TP} + N_{FP}} \tag{17}$$

$$R_{recall} = \frac{N_{TP}}{N_{TP} + N_{FN}} \tag{18}$$

In this paper, the performance of the proposed method is compared and evaluated in terms of accuracy with that of the existing template matching method. Figures 11 and 12 show graphically the measurement results of the accuracy of the two mosaic detection algorithms obtained from (17) and (18). As shown in Figure 11 and Figure 12, the proposed feature projection-based method reduces false detection of the mosaic area, so it can be confirmed that it detects mosaic areas from an image more robustly.

As shown in Figures 11 and 12, it was confirmed that the proposed algorithm used the horizontal and vertical edge projections to detect grid-type mosaic blocks more accurately than the existing method. However, in the case where mosaic blocks are generated in the parts of the input image in which the image quality is degraded, it is possible that the detection accuracy of the proposed method may be decreased. In addition, in this paper, a line edge was used to decrease any error caused by a noise edge. Accordingly, although a noise line edge having a size below a particular size was not automatically considered, any error caused by a noise line edge having a size above that particular size was unavoidable. To solve this issue, it is necessary to either conduct pre-processing such as image smoothing to decrease the noise to the utmost extent possible or adaptively adjust the size of TH_{line} , the threshold determining the line edge, according to the noise inclusion level.

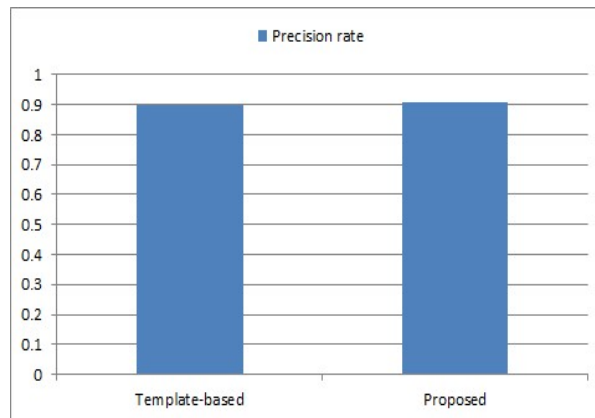


Fig. 11. Precision rates.

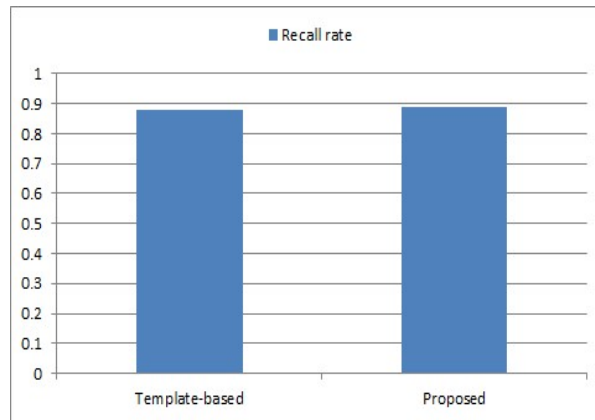


Fig. 10. Recall rates.

Besides, in this paper, as described above, harmful images were selected as the main targets for detecting mosaic regions. Namely, since the images used in the experiments were mostly images that explicitly reveal human body parts or show sexual intercourse performed between a male and a female, it is difficult to include such images as the contents of this paper. Therefore, we selected color images that do not contain these body parts and inserted the input and resulting images into the paper.

6. Conclusion

Recently, as low-priced high-quality cameras are developed and information communication technology makes rapid progress, the types of available video data are diversified. However, such video data sometimes include information not preferred to be exposed to other people such as the face, resident registration number and exposed body part of a person. Accordingly, in the process of uploading a photo or a video on websites or blogs, the face of a person or particular objects are frequently processed with mosaic blocks to protect the portrait rights of a person or to prevent other people from being disgusted. In recent years, there is an increasing need for a new research for effectively detecting a target object region including personal information in an image and blocking the detected object.

In this paper, a new algorithm that more robustly detects the grid-type mosaic blocks from an input image based on the horizontal and vertical line edge projections was proposed. As far as the proposed method is concerned, initially, the Canny edge was extracted from a color image, then the line edges consecutively connected in the horizontal and vertical directions were extracted. Subsequently, the edges in the horizontal and vertical directions were projected, the frequency of the projected edges was calculated, and the candidate mosaic blocks were detected. Subsequently, geometrical features such as size, aspect ratio, and compactness of the detected candidate blocks were used to filter the candidate blocks. Accordingly, non-mosaic

blocks were effectively removed from the candidate mosaic blocks, and the actual mosaic blocks were accurately extracted. In the paper, the experiment results showed that the proposed line edge projection-based method detected grid-type mosaic regions from various types of input color images more robustly than other existing methods.

The proposed grid-type mosaic detection algorithm based on line edge feature projection is expected to be very useful for various practical applications related to video contents such as personal information blocking, video data security, image restoration and post-processing, and harmful image detection. Besides, the proposed grid-type mosaic detection algorithm can be linked to the process of recognizing the detected mosaic region and the procedure of removing the detected mosaic.

In the future, various parameters such as the threshold used in the grid-type mosaic detection algorithm proposed in this paper will be repeatedly tested and adaptively adjusted to enhance the efficiency of the current mosaic detection algorithm. Besides, artificial intelligence-based learning algorithms such as the deep new learning network frequently used nowadays will be used to systematically learn the line edge-based features extracted in this paper and enhance the mosaic block detection accuracy. Also, still and dynamic color images captured in more diverse indoor and outdoor environments will be applied to the proposed algorithm to enhance the robustness of the proposed algorithm.

Acknowledgment. This work was supported by the National Research Foundation of Korea (NRF) grant funded by the Korea government (MSIT) (2019R1F1A1056475)

References

1. Ding, S., Qu, S., Xi, Y., Wan, S.: A Long Video Caption Generation Algorithm for Big Video Data Retrieval. *Future Generation Computer Systems*, Vol. 93, 583-595. (2019)
2. Rim, D., Hasan, M. K., Puech, F., Pal, C. J.: Learning from Weakly Labeled Faces and Video in the Wild. *Pattern Recognition*, Vol. 48, No. 3, 759-771. (2015)
3. Lee, J.-E.: Robust Influenza Analysis Algorithm Based on Image Processing under Varying Radiometric Conditions. *Journal of the Korea Academia-Industrial Cooperation Society*, Vol. 20, No. 7, 127-132. (2019)
4. Cao, Z., Huang, Q., Wu, C.Q.: Maximize Concurrent Data Flows in Multi-radio Multi-channel Wireless Mesh Networks. *Computer Science and Information Systems*, Vol. 17, No. 3, 759-777. (2020)
5. Sun, Z., Lv, Z., Hou, Y., Xu, C., Yan, B.: MR-DFM: A Multi-path Routing Algorithm Based on Data Fusion Mechanism in Sensor Networks. *Computer Science and Information Systems*, Vol. 16, No. 3, 867-890. (2019)
6. Yin, Y., Zhang, W., Xu, Y., Zhang, H., Mai, Z., Yu, L.: QoS Prediction for Mobile Edge Service Recommendation with Auto-encoder. *IEEE Access*, Vol. 7, pp. 62312-62324. (2019)
7. Yin, Y., Xu, W., Xu, Y., Li, H., Yu, L.: Collaborative QoS Prediction for Mobile Service with Data Filtering and SlopeOne Model. *Mobile Information Systems*, vol. 2017, 1-14. (2017)
8. Yin, Y., Chen, L., Xu, Y., Wan, J., Zhang, H., Mai, Z.: QoS Prediction for Service Recommendation with Deep Feature Learning in Edge Computing Environment. *Mobile Networks and Applications*, Vol. 2019, 1-11. (2019)

9. Yin, Y., Aihua, S., Min, G., Xu, Y., Shuoping, W.: QoS Prediction for Web Service Recommendation with Network Location-Aware Neighbor Selection. *International Journal of Software Engineering and Knowledge Engineering*, Vol. 26, No. 4, 611-632. (2016)
10. Yu, J., Kuang, Z., Zhang, B., Zhang, W., Lin, D.: Leveraging Content Sensitiveness and User Trustworthiness to Recommend Fine-Grained Privacy Settings for Social Image Sharing. *IEEE Transactions on Information Forensics and Security*, Vol. 13, No. 5, 1317-1332. (2018)
11. Liu, W., Gao, Y., Ma, H., Yu, S., Nie, J.: Online Multi-Objective Optimization for Live Video Forwarding across Video Data Centers. *Journal of Visual Communication and Image Representation*, Vol. 48, 502-513. (2017)
12. Kim, D.-J.: A Systematic Study of Computer-Based Driving Intervention Program for Elderly Drivers. *Journal of the Korea Academia-Industrial Cooperation Society*, Vol. 20, No. 4, 293-302. (2019)
13. Lee, C.-H., Choi, H.-I.: Algorithm for Improving the Position of Vanishing Point Using Multiple Images and Homography Matrix. *Journal of the Korea Academia-Industrial Cooperation Society*, Vol. 20, No. 1, 477-483. (2019)
14. Lee, J.-S., Oh, M.-K.: Distribution Analysis of Land Surface Temperature about Seoul Using Landsat 8 Satellite Images and AWS Data. *Journal of the Korea Academia-Industrial Cooperation Society*, Vol. 20, No. 1, 434-439. (2019)
15. Wu, D., Zhang, F., Wang, H., Wang, R.: Fundamental Relationship between Node Dynamic and Content Cooperative Transmission in Mobile Multimedia Communications. *Computer Communications*, Vol. 120, 71-79. (2018)
16. Yin, L., Cheng, Q., Wang, Z., Shao, Z.: Big Data for Pedestrian Volume: Exploring the Use of Google Street View Images for Pedestrian Counts. *Applied Geography*, Vol. 63, 337-345. (2015)
17. Flores, A., Belongie, S.: Removing Pedestrians from Google Street View Images. In *Proceedings of the IEEE Computer Society Conference on Computer Vision and Pattern Recognition Workshops*. San Francisco, USA, 53-58. (2010)
18. Guo, D., Tang, J., Cui, Y., Ding, J., Zhao, C.: Saliency-based Content-Aware Lifestyle Image Mosaics. *Journal of Visual Communication and Image Representation*, Vol. 26, 192-199. (2015)
19. Jang, S.-W., Jung, M.: Detection of Harmful Content Using Multilevel Verification in Visual Sensor Data. *Wireless Personal Communications*, Vol. 86, No. 01, 109-124. (2016)
20. Cheng, F., Wang, S.-L., Wang, X.-Z., Liew, A. W.-C., Liu, G.-S.: A Global and Local Context Integration DCNN for Adult Image Classification. *Pattern Recognition*, Vol. 96, 1-12, (2019)
21. Jang, S.-W., Lee, S.-H.: Robust Blocking of Human Faces with Personal Information Using Artificial Deep Neural Computing. *Sustainability*, Vol. 12, No. 6, 1-20. (2020)
22. Park, Y.-J., Lee, J.-W., Choi, G.-S., Park, J.-J.: A Study on Grid Mosaic Detection for Identifying Image Harmfulness. In *Proceedings of the Korea Society of Industrial Information Systems*, 1-5. (2015)
23. Liu, J., Huang, L., Lin, J.: An Image Mosaic Block Detection Method Based on Fuzzy C-Means Clustering. In *Proceedings of the IEEE International Conference on Computer Research and Development*. Shanghai, China, Vol. 1, 237-240. (2011)
24. Wei, Z., Lin, J., Zhang, L., Song, S.: Mosaic Defect Detection Based on Macro Block Solid Edge Detection. *Research Journal of Applied Sciences, Engineering and Technology*, No. 5, Vol. 13, 3549-3553. (2013)
25. Sun, S.-F., Han, S.-H., Wang, G., Xu, Y.-C., Lei, B.-J.: Mosaic Defect Detection in Digital Video. In *Proceedings of the IEEE Chinese Conference on Pattern Recognition*. Chongqing, China, 1-5. (2010)
26. Jang, S.-W., Jung, M.: Robust Detection of Mosaic Regions in Visual Image Data. *Cluster Computing*, Vol. 19, No. 4, 2285-2293. (2016)

27. Yu, J., Zhang, B., Kuang, Z., Lin, D., Fan, J.: iPrivacy: Image Privacy Protection by Identifying Sensitive Objects via Deep Multi-Task Learning. *IEEE Transactions on Information Forensics and Security*, Vol. 12, No. 5, 1005-1016. (2017)
28. Jia, G., Han, G., Rao, H., Shu, L.: Edge Computing-Based Intelligent Manhole Cover Management System for Smart Cities. *IEEE Internet of Things Journal*, Vol. 5, No. 3, 1648-1656. (2018)
29. Zhou, R., Khemmarat, S., Gao, L., Wan, J., Zhang, J.: How YouTube Videos Are Discovered and Its Impact on Video Views. *Multimedia Tools and Applications*, Vol. 75, No. 10, 6035-6058. (2016)
30. Bassel, A., Nordin M. J., Abdulkareem, M. B.: An Invisible Image Watermarking Based on Modified Particle Swarm Optimization (PSO) Algorithm. *International Journal of Security and Its Applications*, Vol. 12, No. 2, 1-8. (2018)
31. Bassel, A., Nordin M. J., Abdulkareem, M. B.: An Invisible Image Watermarking Based on Modified Particle Swarm Optimization (PSO) Algorithm. *International Journal of Security and Its Applications*, Vol. 12, No. 2, 1-8. (2018)
32. Lu, R., Liu, X., Wang, X., Pan, J., Sun K., Waynes, H.: The Design of FPGA-Based Digital Image Processing System and Research on Algorithms. *International Journal of Future Generation Communication and Networking*, Vol. 10, No. 2, 41-54. (2017)
33. Zhou, P., Zhou, Y., Wu, D., Jin, H.: Differentially Private Online Learning for Cloud-Based Video Recommendation with Multimedia Big Data in Social Networks. *IEEE Transactions on Multimedia*, Vol. 18, No. 6, 1217-1229. (2016)
34. Ye, F., Zhang, Z., Chakrabarty, K., Gu, X.: Board-Level Functional Fault Diagnosis Using Multikernel Support Vector Machines and Incremental Learning. *IEEE Transactions on Computer-Aided Design of Integrated Circuits and Systems*, Vol. 33, No. 2, 279-290. (2014)
35. Han, B., Davis, L. S.: Density-Based Multifeature Background Subtraction with Support Vector Machine. *IEEE Transactions on Pattern Analysis and Machine Intelligence*, Vol. 34, No. 5, 1017-1023. (2012)
36. Yan, B., Xiao, L., Zhang, H., Xu, D., Zhang, Y.: An Adaptive Template Matching-Based Single Object Tracking Algorithm with Parallel Acceleration. *Journal of Visual Communication and Image Representation*, Vol. 64, 1-13. (2019)
37. Wang, M., Cui, Q., Sun, Y., Wang, Q.: Photovoltaic Panel Extraction from Very High-Resolution Aerial Imagery Using Region-Line Primitive Association Analysis and Template Matching. *ISPRS Journal of Photogrammetry and Remote Sensing*, Vol. 141, 100-111. (2018)
38. Gaurav, K., Ghanekar, U.: Image Steganography Based on Canny Edge Detection, Dilation Operator and Hybrid Coding. *Journal of Information Security and Applications*, Vol. 41, 41-51. (2018)
39. Shahdoosti, H. R., Rahemi, Z.: Edge-Preserving Image Denoising Using a Deep Convolutional Neural Network. *Signal Processing*, Vol. 159, 20-32. (2019)
40. Zhang, W. C., Zhao, Y. L., Breckon, T. P., Chen, L.: Noise Robust Image Edge Detection Based upon the Automatic Anisotropic Gaussian Kernels. *Pattern Recognition*, Vol. 63, 193-205. (2017)
41. Xu, Q., Varadarajan, S., Chakrabarti, C., Karam, L. J.: A Distributed Canny Edge Detector: Algorithm and FPGA Implementation. *IEEE Transactions on Image Processing*, Vol. 23, No. 7, 2944-2960. (2014)
42. Lee, J., Tang, H., Park, J.: Energy Efficient Canny Edge Detector for Advanced Mobile Vision Applications. *IEEE Transactions on Circuits and Systems for Video Technology*, Vol. 28, No. 4, 1037-1046. (2018)
43. Jiang, N., Yang, W., Duan, L., Xu, X., Liu, Q.: Acceleration of CT Reconstruction for Wheat Tiller Inspection Based on Adaptive Minimum Enclosing Rectangle. *Computers and Electronics in Agriculture*, Vol. 85, 123-133. (2012)

44. Kwak, E., Habib, A.: Automatic Representation and Reconstruction of DBM from LiDAR Data Using Recursive Minimum Bounding Rectangle. *ISPRS Journal of Photogrammetry and Remote Sensing*, Vol. 93, 171-191. (2014)
45. Lei, Y., Zheng, L., Huang, J.: Geometric Invariant Features in the Radon Transform Domain for Near-Duplicate Image Detection. *Pattern Recognition*, Vol. 47, No. 11, 3630-3640. (2014)
46. Gang, L., Li, X.-H., Zhou, J.-L., Gong X.-G.: Geometric Feature-based Facial Expression Recognition Using Multiclass Support Vector Machines. In *Proceedings of the IEEE International Conference on Granular Computing*. Nanchang, China, 318-321. (2019)
47. Wang, L., Xu, F., Hagiwara, I.: Investigation into Registration of Scanned 3D Image Based on Geometric Feature Identification. In *Proceedings of the International Conference on Computer Supported Cooperative Work in Design*, 648-653. (2009)
48. Zhang, L., Zhang, D., Sun, M.-M., Chen, F.-M.: Facial Beauty Analysis Based on Geometric Feature: Toward Attractiveness Assessment Application. *Expert Systems with Applications*, Vol. 82, 252-265. (2017)
49. Lang, H., Wu, S.: Ship Classification in Moderate-Resolution SAR Image by Naive Geometric Features-Combined Multiple Kernel Learning. *IEEE Geoscience and Remote Sensing Letters*, Vol. 14, No. 10, 1765-1769. (2017)
50. Ballihi, L., Amor, B. B., Daoudi, M., Srivastava, A., Aboutajdine, D.: Boosting 3-D-Geometric Features for Efficient Face Recognition and Gender Classification. *IEEE Transactions on Information Forensics and Security*, Vol. 7, No. 6, 1766-1779. (2012)
51. Jin, L., Zhang, W., Ma, G., Song, E.: Learning Deep CNNs for Impulse Noise Removal in Images. *Journal of Visual Communication and Image Representation*, Vol. 62, 193-205. (2019)
52. Giannatou, E., Papavieros, G., Constantoudis, V., Papageorgiou, H., Gogolides E.: Deep Learning Denoising of SEM Images Towards Noise-Reduced LER Measurements. *Microelectronic Engineering*, Vol. 216, 1-8. (2019)
53. Chen, R., Zhao, F., Yang, C., Li, Y., Huang T.: Robust Estimation for Image Noise Based on Eigenvalue Distributions of Large Sample Covariance Matrices. *Journal of Visual Communication and Image Representation*, Vol. 63, 1-10. (2019)
54. Xu, J., Zhang, P., Yang, Z., Gao, Z., Nie, K., Ma, J.: Image Lag Elimination Algorithm for Pulse-Sequence-Based High-Speed Image Sensor. *IEEE Access*, Vol. 7, 159575-159583. (2019)
55. Bohat, V. K., Arya, K. V.: A New Heuristic for Multilevel Thresholding of Images. *Expert Systems with Applications*, Vol. 117, 176-203. (2019)
56. Elaziz, M. A., Lu, S.: Many-Objectives Multilevel Thresholding Image Segmentation Using Knee Evolutionary Algorithm. *Expert Systems with Applications*, Vol. 125, 305-316. (2019)
57. Chakraborty, F., Nandi, D., Roy, P. K.: Oppositional Symbiotic Organisms Search Optimization for Multilevel Thresholding of Color Image. *Applied Soft Computing*, Vol. 82, 1-19. (2019)
58. Talukder, A., Alam, M. G. R., Tran, N. H., Niyato, D., Park, G. H., Hong, C. S.: Threshold Estimation Models for Linear Threshold-Based Influential User Mining in Social Networks. *IEEE Access*, Vol. 7, 105441-105461. (2019)
59. Zhang, X., Feng, X., Xiao, P., He, G., Zhu, L.: Segmentation Quality Evaluation Using Region-Based Precision and Recall Measures for Remote Sensing Images. *ISPRS Journal of Photogrammetry and Remote Sensing*, Vol. 102, 73-84. (2015)
60. Ziolkowski, B.: Fuzzy Precision and Recall Measures for Audio Signals Segmentation. *Fuzzy Sets and Systems*, 279, 101-111. (2015)
61. Bautista-Gomez, L., Benoit, A., Cavelan, A., Raina, S. K., Sun, H.: Coping with Recall and Precision of Soft Error Detectors. *Journal of Parallel and Distributed Computing*, Vol. 98, 8-24. (2016)

62. Hassler, E. E., Hale, D. P., Hale, J. E.: A Comparison of Automated Training-by-Example Selection Algorithms for Evidence-Based Software Engineering. *Information and Software Technology*, Vol. 98, 59-73. (2018)
63. Thara, D.K., PremaSudha, B.G., Fan, X.: Epileptic Seizure Detection and Prediction Using Stacked Bidirectional Long Short Term Memory. *Pattern Recognition Letters*, Vol. 128, 529-535. (2019)

Seok-Woo Jang received his B.S., M.S., Ph.D. degrees in Computer Science from Soongsil University, Seoul, Korea, in 1995, 1997, and 2000, respectively. From October 2003 to January 2009, he was a Senior Researcher with the Construction Information Research Department at Korea Institute of Construction Technology (KICT), Ilsan, Korea. Since March 2009, he has been a Professor in the Department of Digital Media, Anyang University, Korea. His primary research interests include robot vision, augmented reality, video indexing and retrieval, biometrics and pattern recognition.

Received: February 27, 2020; Accepted: January 06, 2021.